SEISMIC RESPONSE OF BURIED PIPELINES
TO SURFACE WAVE PROPAGATION EFFECTS

P. Shi[1], T.D. O'Rourke[2], Y. Wang[3], K. Fan[1]

[1]*Geotechnical Engineer, Geotechnical and Tunneling Group, PB Americas, Inc., New York, NY, USA*
[2]*Professor, School of Civil & Environmental Engineering, Cornell University, Ithaca, NY, USA*
[3]*Professor, Department of Building and Construction, City University of Hong Kong, Hong Kong, China*
Email: Ship@pbworld.com, TDO1@cornell.edu, Yuwang@cityu.edu.hk, Fank@pbworld.com

ABSTRACT:
This paper describes an analytical model for seismic response of buried pipelines to surface wave propagation effects. This model accounts for the mechanism of shear transfer and relative joint pullout movement as a result of soil-structure interaction. Finite element simulation of the performance of jointed concrete cylinder pipelines (JCCPs) under surface wave propagation effects during the 1985 Michoacan earthquake is consistent with the field observations. In conjunction with the work conducted by Wang (2006) at Cornell University on body wave effects, a dimensionless plot is developed for estimating the relative joint pullout movement of JCCPs. The application of the dimensionless plot is expanded to other types of pipelines composed of joints exhibiting ductile tensile failure behavior, such as cast iron (CI) pipelines with lead-caulked joints, by incorporating a dimensionless reduction factor to consider the joint ductility.

KEY WORDS:
Soil-Structure Interaction, Surface Waves, Joint Pullout, Finite Element Methods, Jointed Concrete Cylinder Pipelines, Cast Iron Pipelines

1. INTRODUCTION

Soil-structure interaction triggered by seismic waves has an important effect on buried pipeline behavior, and when integrated over an entire network of pipelines, on system performance (O'Rourke, et al. 2004a). In general, there are two types of seismic waves, body and surface waves. Compared with body waves, surface waves have a much lower apparent wave propagation velocity, which drives higher ground strain. Under the appropriate conditions, therefore, surface waves can be more hazardous to buried pipelines than body waves. Severe damage to water supply pipelines related to surface wave propagation effects has been recorded during previous earthquakes, such as the 1985 Michoacan earthquake in Mexico City (Ayala and O'Rourke, 1989).

One method for estimating pipeline damage in future earthquakes is to develop regressions between observed repair rates during previous earthquakes and measured seismic parameters (O'Rourke, et al. 2004a and b). Because of the limited data regarding damage to buried pipelines under the effects of surface waves, it is useful to develop analytical models that can provide insight about the mechanism of the soil-structure interaction under surface wave effects. This paper describes an analytical model to analyze the joint pullout movement of buried pipelines under surface wave traveling effects. Following the Introduction, the surface wave characteristics are briefly described in Section 2. The mechanism of buried pipeline interaction to surface wave propagation effects is explored in Section 3. FE simulation of the performance of jointed concrete cylinder pipelines (JCCPs) during the 1985 Michoacan earthquake is discussed in Section 4. A dimensionless chart is developed to facilitate the estimate of the joint pullout movement of JCCPs under the effects of seismic waves. The application of the dimensionless plot is expanded in Section 5 to other types of pipelines composed of joints exhibiting ductile tensile failure behavior, such as cast iron (CI) pipelines with lead-caulked joints.

While buried pipelines can exhibit both relatively rigid and flexible behaviors under surface wave propagation effects, this paper focuses on the behaviors of relatively rigid pipelines. The behaviors of relatively flexible pipelines can be referred to O'Rourke et al. (2004b) and Wang et al. (2006).

2. SURFACE WAVE CHARACTERISTICS

Surface waves are generated by the reflection and refraction of body waves, and travel along the ground surface. Two major types of surface waves are Love (L-) and Rayleigh waves (R-waves). The R-waves generate alternating compressive and tensile axial strains along pipelines. The L-waves generate bending strains in pipelines that are typically 2 to 3 orders of magnitude less than the axial strains induced by R-waves. As such, only the effects of R-waves are discussed in this paper.

Body wave reflection and refraction in large, sedimentary basins (several km wide with soil depths ≤ 1 km) can cause R-waves that amplify the ground motion significantly (O'Rourke, 1998). The amplification effects associated with R-wave propagation can be demonstrated by the two strong motion records, as shown in Fig.1, collected in Mexico City during the 1985 Michoacan earthquake (Ayala and O'Rourke, 1989). The strong motion station, Ciudad Universitaria - Lab, is located in the Hill Zone, outside of the sedimentary basin, and was affected mainly by body waves. The strong motion station, Central de Abastos - Oficinas, is located in the Lake Zone, inside the sedimentary basin, and was affected mainly by surface waves. In the Hill Zone record (Fig. 1a), the peak ground velocity (PGV) is about 10 cm/sec, occurred roughly at 20 to 30 seconds after initial measurement triggering. The ground motion died out at approximately 60 seconds after initial triggering. In the Lake Zone record (Fig. 1b), the PGV associated with surface waves was higher than 30 cm/sec that occurred about 60 and 90 seconds after initial triggering. The PGV remained as high as 15 cm/sec at 140 seconds after initial triggering. The surface waves were similar to sinusoidal waves with similar amplitude and predominant period that can be estimated as about 3.5 seconds. The phase velocity of the surface waves was estimated as 120 m/sec corresponding to the predominant period of 3.5 seconds based on the dispersion curves developed for this station by Ayala and O'Rourke (1989). Comparison between Figs. 1a and b shows that the surface wave generation and propagation increase the peak amplitudes and prolong the duration of transient ground deformation significantly.

The seismic loads on buried pipelines imposed by wave propagation are typically characterized by ground strains. The ground strain, ε_g, can be calculated as the ratio of ground particle velocity, V, to apparent wave propagation velocity, C_a, as $\varepsilon_g = V/C_a$. For surface waves, the apparent wave propagation velocity, C_a, is equal to the phase velocity, C_{ph}, since surface waves travel along the ground surface. To calculate the ground strain along the axial direction of a pipeline, it is necessary to resolve the ground particle and apparent wave propagation velocities into components parallel to the pipeline. For a pipeline orientated at an angle, α, with respect to the particle velocity, V, as shown in Fig. 2, the ground strain along the pipe axial direction can be calculated as

$$\varepsilon_g = \frac{V\cos\alpha}{C_a/\cos\alpha} = \frac{V}{C_a}\cos^2\alpha = \frac{V}{C_{ph}}\cos^2\alpha \qquad (2.1)$$

The ground strain along the pipe axis reaches its maximum value, V/C_{ph}, when the pipeline is in parallel to the ground particle and phase velocities of surface waves.

3 SURFACE WAVE INTERACTION WITH PIPELINES

As discussed by O'Rourke et al. (2004b), for an incremental section of continuous buried pipeline, dx, subjected a surface wave, simplified as a sinusoidal wave with maximum amplitude of ground strain $\varepsilon_{mg} = V_p/C_{ph}$, where V_p is peak ground particle velocity and C_{ph} is the phase velocity along the pipe axial direction, the rate of pipe strain, ε_p, accumulation is given by

$$d\varepsilon_p/dx = f/EA \qquad (3.1)$$

where f is the shear transfer between pipe and soil in unit pipe length, E is pipe material modulus, A is pipe cross-sectional area, and EA is pipe axial stiffness. The rate of ground strain, ε_g, accumulation is given by

a) Ciudad Universitaria – Lab (Hill Zone)

PGV over 30 cm/sec from R-waves

T = 21/6 =3.5 Sec

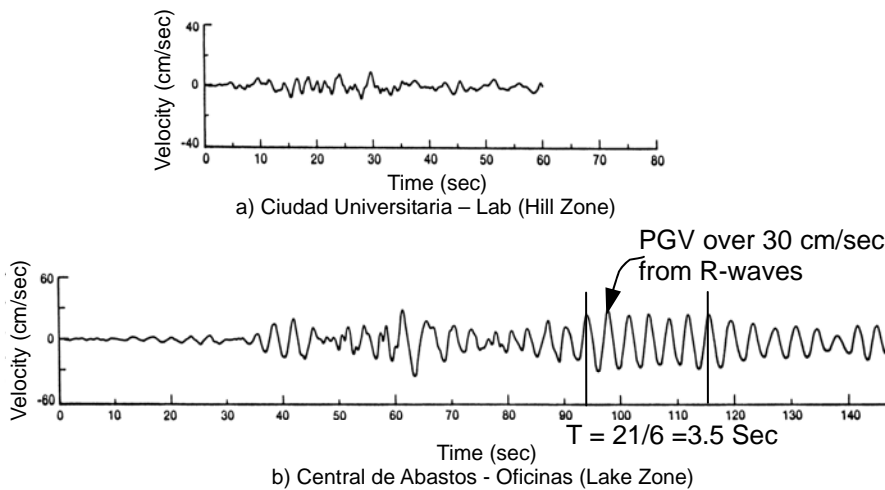b) Central de Abastos - Oficinas (Lake Zone)

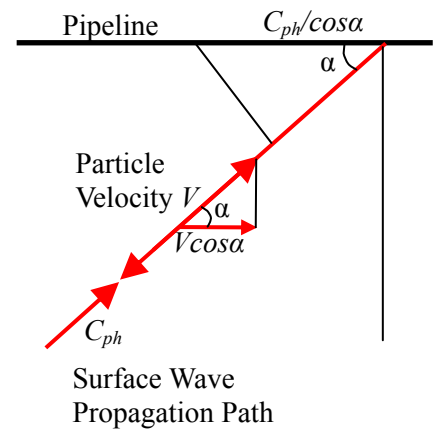Figure 1 Strong Motion Velocity Histories during the 1985 Michoacan Earthquake (after Ayala and O'Rourke, 1989)

Figure 2 Resolution of Particle and Phase Velocities of R-Waves Along the Pipeline Axial Direction

$$\frac{d\varepsilon_g}{dx} = \frac{d}{dx}\left(\frac{V}{C_{Ph}}\right) \qquad (3.2)$$

in which V is the ground particle velocity.

Figure 3 shows the seismic response of a continuous pipeline with a locally weak joint under the action of a surface wave. When surface waves propagate along the pipeline, the ground deformation transfers shear force to the pipeline. Because of the relatively low phase velocity of surface waves, the strain accumulation rate of ground soil is generally higher than that of the pipeline so that the pipeline is not able to deform in unison with the ground soil. The shear transfer is shown in Fig. 3a with small arrows indicating its direction. The axial force in the pipeline is the integration of the shear transfer along the pipe axis. The axial force increases from zero where the ground strain is zero to its maximum value $f*(\lambda/4)$ after a quarter of wavelength of shear accumulation. When the maximum tensile force in the pipeline exceeds the tensile capacity of the locally weak joint, the joint will be cracked, and the axial tensile force at the pipe ends, connected with the joint, is assumed to drop to zero.

Figure 4 shows the seismic response of the continuous pipeline with a cracked joint under the action of a surface wave. When the axial tensile force at the cracked joint drops to zero, the pipeline sections at both ends of the cracked joint tend to move away from each other. The ground at the cracked joint has zero displacement as shown in Fig. 4b. In the vicinity of the cracked joint, the pipe displacement is larger than the ground displacement and the shear transfer from the ground to pipeline tries to prevent the pipeline sections from moving away from each other until the ground displacement equals the pipe displacement at point A. Beyond point A, the ground displacement is larger than the pipe displacement and the shear transfer direction reverses. The integration of the differential strain between pipeline and soil from the cracked joint to the shear transfer reversal point, A, is represented by half of the shaded area in Fig. 4b. It is the relative displacement between the pipeline and ground at the cracked joint, which equals to one half of the relative joint displacement.

For seismic wave interaction with pipelines, the relative joint pullout displacement is determined by soil-structure interaction and cannot be solved by analytical methods. Finite element (FE) methods are used to model the surface wave interaction with a particular type of pipeline, JCCPs, in the next section.

4   FINITE ELEMENT SIMULATION OF SURFACE WAVE INTERACTION WITH JCCPS

In this work the term JCCPs is used to represent pipelines composed of reinforced concrete and steel cylinders that are coupled with mortared, rubber-gasket bell-and-spigot joints. Severe damage to JCCPs has been reported
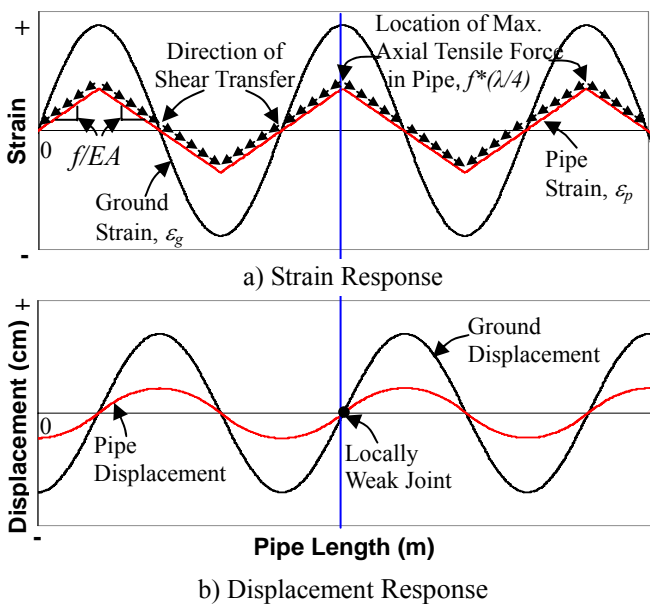
a) Strain Response

b) Displacement Response

Figure 3 Sinusoidal Wave Interaction with a Continuous Relatively Rigid Pipeline
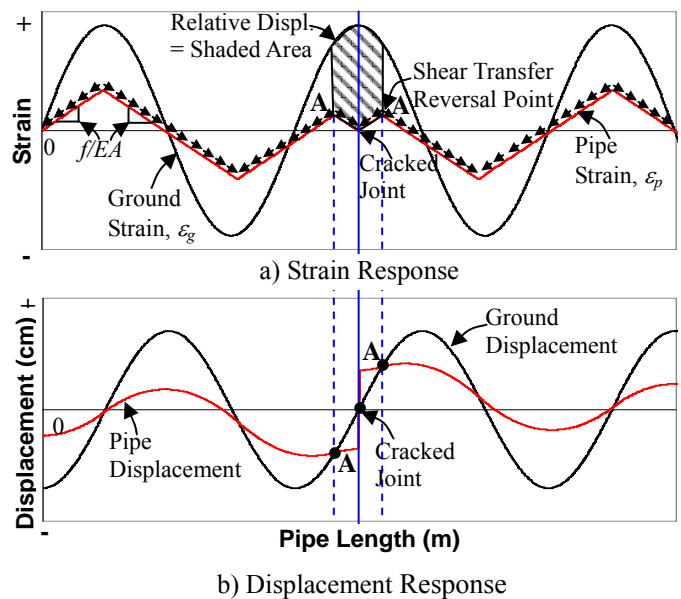

a) Strain Response

b) Displacement Response

Figure 4 Sinusoidal Wave Interaction with a Relatively Rigid Pipeline with a Cracked Joint

during previous earthquakes. For example, Ayala and O'Rourke (1989) reported significant repairs in JCCPs after the 1985 Michoacan earthquake. There were 60 repairs, concentrated at the joints, in Federal District JCCP transmission lines, resulting in a relatively high repair rate of 1.7 repair/km. Ayala and O'Rourke (1989) pointed out that most of the water system damage was due to seismic wave propagation effects.

4.1 JCCP Characteristics

As discussed by O'Rourke et al. (2004b), the performance of JCCPs is affected by rubber-gasket bell-and-spigot connections. The rubber gasket is often 18 to 22 mm wide when compressed to form a water-tight seal. Cement mortar is poured in the field to further seal the joint. The pullout capacity of the joint, in terms of axial slip to cause leakage, depends on how much movement can occur before the rubber gasket loses its compressive seal. The design and as-built drawings examined by O'Rourke et al. (2004b) show that between 15 and 60 mm of axial movement is typically required to pull the gasket out of the horizontal portion of the bell into the flared end adjacent to the mortar filling. Most frequently, the slip capacity is 25 mm. This axial slip can be regarded as an as-designed capacity before the loss of gasket compression is initiated. This capacity will vary according to the workmanship during installation and subsequent movements of the pipeline. The pullout resistance of the joints is also affected by the tensile behavior of the cement mortar at the joints. It is not uncommon for the mortar at the JCCP joints to be cracked and separated as a result of shrinkage during cure as well as subsequent operational loads and movement in the field.

4.2 Finite Element Simulation

FE analyses of surface wave interaction with JCCPs were performed using the program BSTRUCT (Chang, 2006). The pipeline was modeled with beam column elements that were connected to the ground by spring-slider elements capable of representing shear transfer as an elasto-plastic process. The locally weak joint in the JCCP was modeled as a spring-slider element with a zero length and very low axial pullout resistance that for modeling purposes can be taken as negligible. The FE model was composed of 1666 pipe elements and 1669 spring slider elements over a distance of roughly 10 km for an average element length of 6 m.

The strong motion recording at Central de Adastos - Oficinas (Lake Zone) in the north-south direction during the 1985 Michoacan earthquake in Mexico City, as shown in Fig. 1b, was used as ground motion input. Time records of strong motion were converted to displacement versus distance records by assuming that $x = C_{Ph}t$, in

which x is distance, t is time from the strong motion recording. The phase velocity, C_{Ph}, is taken as 120 m/sec and the predominant period is 3.5 seconds. The seismic displacement versus distance record was superimposed on the spring-slider elements, which then conveyed ground movement to pipeline by means of the elasto-plastic properties used to characterize the spring-sliders. When the maximum slope of the displacement versus distance record (corresponding to maximum ground particle velocity in the velocity record) was superimposed on the weak pipeline joint, the maximum axial slip of the joint was calculated.

The FE analysis was used to evaluate the performance of the 1829-mm-(72 in.)-diameter jointed concrete Federal District transmission line in Mexico City, which was severely damaged during the 1985 Michoacan earthquake due to R-wave propagation effects (Ayala and O'Rourke, 1989). It was assumed that the pipeline is orientated in parallel with the direction of wave propagation, which results in the maximum joint pullout movement. Figure 5 shows the displacement and strain of ground soil and pipeline in the vicinity of the locally weak joint. The pipeline exhibits relatively rigid behavior and is not able to deform in unison with the ground soil. The relative joint displacement is the shaded area and is calculated as 16 cm. The high predicted relative joint displacement indicates a strong potential for joint pullout and disengagement of JCCPs under surface wave effects and is consistent with field observations.

4.3 Dimensionless Plot

Parametric studies are performed to different pipe properties, seismic wave characteristics, and ground conditions. The results of the parametric studies, in conjunction with the work performed by Wang (2006) on body wave effects, are summarized in Fig. 6 with two dimensionless parameters, δ/δ_0 and f/EAR.

The parameter δ_0 is defined as the area under the seismic sinusoidal ground strain pulse and can be calculated by $\delta_0 = V_pT/\pi$, where T is the predominant period of the seismic wave. The dimensionless parameter, δ/δ_0, indicates the relative joint displacement normalized with respect to a displacement index of the seismic wave characteristics. The parameter R is defined as the ratio of V_p/C_a to the raise distance, $\lambda/4$, i.e. $R = (V_p/C_a)/(\lambda/4)$ where λ is the wave length equal to the product of the apparent wave propagation velocity, C_a, and predominate period, T, of seismic waves. The dimensionless parameter, f/EAR, represents a combination of key ground conditions, pipeline properties, and seismic wave characteristics.

Wang et al. (2006) proposed a criterion to determine if a pipeline is either axially flexible or rigid based on the value of f/EAR. When $f/EAR \geq 1$, the pipeline is relatively flexible with respect to ground deformation induced by seismic waves. When $f/EAR < 1$, the pipeline is relatively rigid with respect to ground deformation. When affected by body waves, pipelines generally exhibit relatively flexible behavior because the high apparent wave velocity drives the ground strain accumulation rate to lower than the pipeline strain accumulation rate. When affected by surface waves, pipelines can be either relatively flexible or rigid. The behaviors of a relatively flexible pipeline under seismic wave effects can be referred to O'Rourke et al. (2004b) and Wang et al. (2006).

With known ground conditions, pipeline properties, and seismic wave characteristics, the values of f/EAR and δ_0 can be calculated and joint displacement, δ, can be estimated directly using Fig. 6. This chart can be used to facilitate the computation of the joint pullout movement of virtually any conventional JCCPs affected by seismic waves. Examples of the application of the dimensionless plot can be referred to Wang et al. (2006).

5   MODEL APPLICATION TO CI PIPELINES

In previous sections, an analytical model is developed for seismic wave response of JCCPs. In this section, this model is expanded to analyze seismic wave response of CI pipelines composed of lead-caulked joints.

5.1 CI Pipeline Characteristics

CI pipeline is one of the oldest and most commonly used pipelines for water and gas transportation in North America. The detailed descriptions of the characteristics of CI pipelines can be referred to Shi (2006). Typically,
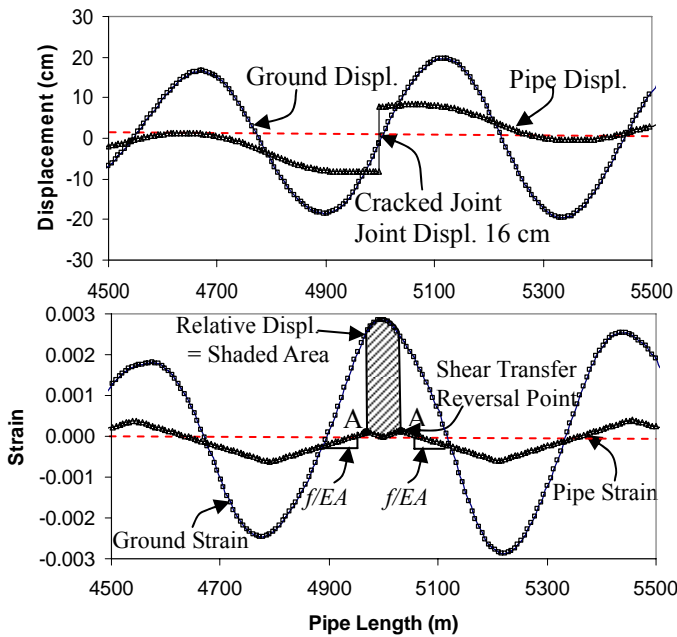
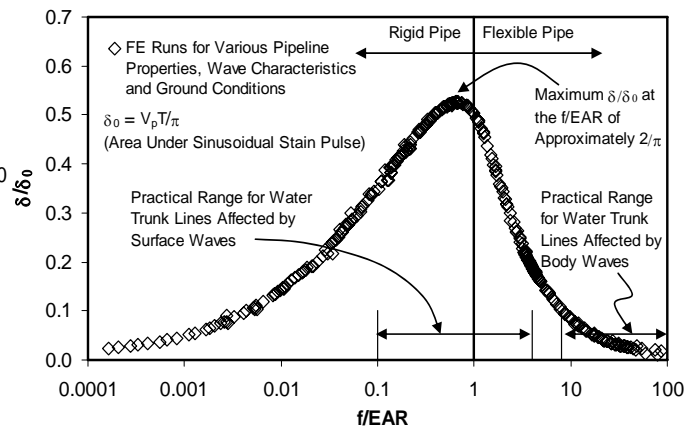Figure 5 FE Simulation of JCCP Response to Surface Wave Propagation Effects

Figure 6 Dimensionless Plot Between δ/δ_0 and f/EAR

CI pipe segments are connected by lead-caulked joints. In contrast to the JCCP joints of which the tensile capacity drops to zero after cracking, the lead-caulked joints of CI pipelines show an elasto-plastic tensile behavior. Under tension, a very small axial displacement, 0 to 2.5 mm, is needed to mobilize the full axial tensile capacity of lead-caulked joints. The joint tensile capacity remains approximately constant with additional movement after it is mobilized. The pullout capacity of the joint in terms of axial slip to cause leakage depends on how much movement can occur before the lead caulking loses its compressive seal. Based on the laboratory test data, Untrauer et al. (1970) reported that, after an initial period of very small leakage, the lead-caulked joints can sustain an axial slip from 25 to 50 mm without further loss of water.

5.2 Seismic Wave Interaction with CI Pipelines

Figure 7 illustrates the seismic response of a CI pipeline with lead-caulked joints. It is assumed that there is a locally weak joint in the pipeline and the pipeline on either side of the weak joint behaves as a continuous one. The strain at the pipe ends connected with the weak joint is controlled by the tensile capacity of the joint and is equal to $\varepsilon_p = F_J/EA$, where F_J is the joint tensile capacity and EA is the axial stiffness of the pipeline. As a wave passes across the joint, strain in the continuous pipeline on both sides of the weak joint accumulates linearly from $\varepsilon_p = F_J/EA$ at a slope of f/EA until the reversal of the relative displacement (point A in Fig. 7), after which pipe strain accumulates at the same slope but with opposite direction. There is no relative displacement between pipe and ground at point A where the reversal of relative displacement occurs. The relative joint pullout displacement is equal to the shaded area in Fig. 7.

Comparison between Figs. 4b and 7 shows that the difference between the seismic response of the JCCP and CI pipeline is that the strain begins to accumulate from $\varepsilon_p = 0$ for the JCCP and from $\varepsilon_p = F_J/EA$ for the CI pipeline. The difference results from the different tensile behaviors between the rubber-gasket bell-and-spigot and lead-caulked joints in the JCCP and CI pipeline, respectively. The JCCP joint has a brittle tensile failure behavior, which can provide zero tensile resistance after it cracks. The CI joint has a ductile tensile failure behavior, which remains its tensile capacity approximately constant with additional movement after it is mobilized. In this study, the term, brittle joint, is used for a joint with a brittle tensile failure behavior, and ductile joint is used for a joint with a ductile tensile failure behavior. The brittle joint can be treated as a special case of the ductile joint, which has zero joint capacity, $F_J = 0$.
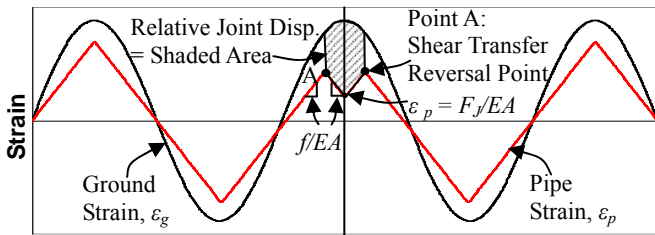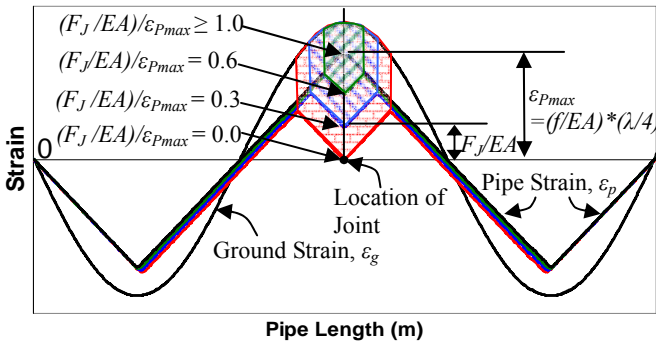
Figure 7 Sinusoidal Wave Interaction with CI Pipeline

Figure 8 Strain Response Curve for a Relatively Rigid Pipeline with Different Values of $(F_J/EA)/\varepsilon_{Pmax}$
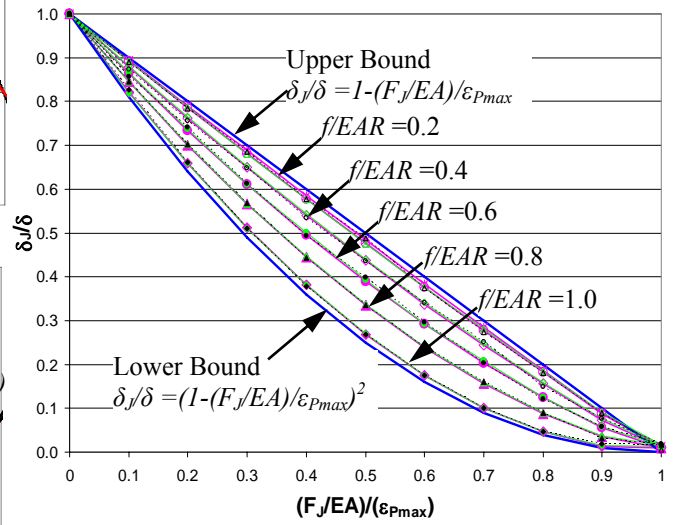

Figure 9 Reduction Curves from FE Analysis Results

5.3 Relative Joint Displacement Reduction Curves

Figure 8 shows the strain response of a relatively rigid pipeline with a ductile joint with different tensile capacities. In this figure, the joint capacity is expressed as a dimensionless parameter, $(F_J/EA)/\varepsilon_{Pmax}$, in which F_J/EA is the strain at the pipe ends connected with the joint, and ε_{Pmax} is the maximum possible strain at the pipe ends with a value of $(f/EA)*\lambda/4$. The maximum pipe strain, ε_{Pmax}, occurs when the axial stiffness of the joint is equal to or higher than that of the pipeline. The parameter $(F_J/EA)/\varepsilon_{Pmax}$ represents a normalized strain at the pipe ends, connected with the joint, from which the pipe strain begins to accumulate. For a brittle joint, which has zero joint capacity after cracked, strain at the pipe ends begins to accumulate from zero, resulting in the largest relative joint displacement. With the increase of joint capacity, $(F_J/EA)/\varepsilon_{Pmax}$ increases, and the relative joint displacement decreases. When $(F_J/EA)/\varepsilon_{Pmax}$ is equal to or larger than 1, strain at the pipe ends is equal to the maximum possible pipe strain and cannot increase any more. The relative joint displacement is zero if the pipeline elastic elongation is neglected. Because the relative joint displacement reaches its maximum value when the joint capacity is zero, i.e. brittle joint case, the displacement of a ductile joint, δ_J, can be normalized with respect to the displacement of a brittle joint, δ, and expressed as a dimensionless parameter, δ_J/δ.

Figure 9 summarizes the relationship between δ_J/δ and $(F_J/EA)/\varepsilon_{Pmax}$ from 150 runs of FE analyses for 3 different pipeline and wave combinations. For each pipe and wave combination, the Young's modulus, E, of pipe material was varied artificially and 5 different f/EAR values were obtained. For each f/EAR value, 10 FE analyses were performed by varying the joint capacity with $(F_J/EA)/\varepsilon_{Pmax}$ values ranging from 0 to 1. Because the curves in Fig. 9 show the reduction of the relative displacement for ductile joints with respect to brittle joints, they are called relative joint displacement reduction curves in this study. Figure 9 shows that all the reduction curves are bounded by an upper bound, $\delta_J/\delta = 1- (F_J/EA)/\varepsilon_{Pmax}$, and a lower bound, $\delta_J/\delta = (1-(F_J/EA)/\varepsilon_{Pmax})^2$. When the f/EAR value is equal to or larger than 1, the reduction curves converge to the lower bound. With the decrease of the f/EAR value, the reduction curves move from the lower to upper bound. When the f/EAR value is equal to or less than 0.2, the reduction curves converge to the upper bound. For different pipeline and seismic wave combinations, if their f/EAR values are same, they share the same reduction curve.

Combining the dimensionless plot provided in Fig. 6 and the reduction curves shown in Fig. 9, it is possible to estimate the joint displacement of virtually any pipeline with either brittle or ductile joints under the effects of seismic waves. The application of Fig. 9 in combination of Fig. 6 can be referred to Shi (2006).

6. CONCLUSIONS

This paper describes an analytical model for buried pipeline response to surface wave propagation effects. When surface waves propagate along buried pipelines, the pipelines generally exhibit a relatively rigid behavior and are not able to deform in unison with the ground soil. FE analyses predicted a relative joint displacement of 16 cm for a-1829-mm-diameter JCCP under the action of the surface waves recorded during the 1985 Michoacan earthquake in Mexico City. The high predicted relative joint displacement indicates a strong potential of joint pullout and disengagement when the JCCP is affected by surface waves. In conjunction with Wang's work (2006) on body wave effects, a dimensionless chart that incorporates the key parameters on pipeline properties, ground conditions, and wave characteristics is developed based on 320 runs of FE simulations. This chart can be used to facilitate the computation of the joint pullout movement of virtually any conventional JCCPs affected by seismic waves.

The analytical model is applied to other types of pipelines, such as CI trunk and distribution mains with lead-caulked joints that have ductile pullout characteristics. The ductility of joint reduces the joint pullout displacement compared with joints with brittle pullout characteristics, such as the JCCP joints. The reduction of the relative joint displacement can be estimated using dimensionless reduction curves developed on the basis of 150 runs of FE simulations. By using the dimensionless chart and reduction curves together, it is able to estimate the joint pullout displacement of CI pipelines under the effects of virtually any seismic waves.

ACKNOWLEDGMENTS

REFERENCES

1. Ayala, A.G. and O'Rourke, M.J. (1989). Effects of the 1985 Michoacan Earthquake on Water System and Other Buried Lifelines in Mexico City. *Technical Report NCEER-89-0009*, MCEER, Buffalo, NY, Mar. 1989.
2. Chang, J.F. (2006). P-Y Modeling of Soil-Pile Interaction. Ph.D. Dissertation, School of Civil & Environmental Engineering, Cornell University, Ithaca, NY.
3. O'Rourke, T.D. (1998). An Overview of Geotechnical and Lifeline Earthquake Engineering. Geotechnical Special Publication No. 75, ASCE, Reston, VA. *Proceedings of Geotechnical Earthquake Engineering and Soil Dynamics Conference*. Seattle, WA, Vol. 2, 1392-1426.
4. O'Rourke, T.D., Wang, Y., and Shi, P. (2004a). Advances in Lifeline Earthquake Engineering. *Proceedings of 13ᵗʰ World Conference on Earthquake Engineering*, Vancouver, British Columbia, Canada, Aug., 2004, Paper No. 5003.
5. O'Rourke, T.D., Wang, Y., Shi, P., and Jones, S. (2004b). Seismic Wave Effects on Water Trunk and Transmission Lines. *Proceedings of the 11ᵗʰ International Conference on Soil Dynamics & Earthquake Engineering and 3ʳᵈ International Conference on Earthquake Geotechnical Engineering, Berkeley*, CA, Vol. 2, 420-428.
6. Shi, P. (2006). Seismic Response Modeling of Water Supply Systems. Ph.D. Dissertation, Cornell University, Ithaca, NY.
7. Untrauer, R.E., Lee, T.T., Sanders W.W., and Jawad, M.H. (1970). Design Requirements for Cast Iron Soil Pipe. *Bulletin 199*, Iowa State University, Engineering Research Institute, 60-109.
8. Wang, Y. (2006). Seismic Performance Evaluation of Water Supply Systems. Ph.D. Dissertation, Cornell University, Ithaca, NY.
9. Wang, Y., O'Rourke, T.D., and Shi, P. (2006). Seismic Wave Effects on the Longitudinal Forces and Pullout of Underground Lifelines. *Proceedings of the 100ᵗʰ Anniversary Earthquake Conference: Commemorating the 1906 San Francisco Earthquake*, San Francisco, California, April 18-22, 2006